Dalton Transactions

ROYAL SOCIETY OF CHEMISTRY

PAPER

View Article Online
View Journal | View Issue

Check for updates

Cite this: *Dalton Trans.*, 2022, **51**, 15771

Indium(III)/2-benzoylpyridine chemistry: interesting indium(III) bromide-assisted transformations of the ligand†

Christina Stamou,[a] Zoi G. Lada,[b] Christos T. Chasapis,[c] Dionissios Papaioannou,*[a] Pierre Dechambenoit*[d] and Spyros P. Perlepes*[a,b]

Reactions of 2-benzoylpyridine, (py)(ph)CO, with InX_3 (X = Cl, Br) in EtOH at room temperature have been studied. The $InCl_3$/(py)(ph)CO system has provided access to complex $[InCl_3\{(py)(ph)CO\}(EtOH)]\cdot\{(py)(ph)CO\}$ (**1**) and the byproduct {(pyH)(ph)CO}Cl (**2**). The reaction of $InBr_3$ with (py)(ph)CO has led to a mixture of (L)$[InBr_4\{(py)(ph)CO\}]$ (**3**) and $[In_2Br_4\{(py)(ph)CH(O)\}_2(EtOH)_2]$ (**4**), where L^+ is the 9-oxo-indolo[1,2-*a*]pyridinium cation and $(py)(ph)CH(O)^-$ is the anion of (pyridin-2-yl)methanol. Based on solubility and crystallisation time differences between the two components of the mixture, complex **4** was isolated in pure form, *i.e.* free from **3**. The formations of the counterion L^+ and the coordinated $(py)(ph)CH(O)^-$ anion represent clearly $InBr_3$-promoted/assisted transformations. Reaction mechanisms have been proposed for the formation of **2**, **3** and **4**. Complex **4** could also be isolated by the reaction of $InBr_3$ and pre-formed (py)(ph)CH(OH) in EtOH. The solid-state structures of **1**, **3** and **4** were determined by single-crystal X-ray crystallography, while the identity of the salt **2** was confirmed by microanalyses and a variety of spectroscopic techniques, including ESI-MS spectra. In the indium(III) complexes, the metal ions are 6-coordinate with a distorted octahedral geometry. The halogeno groups (Cl^-, Br^-) in the three complexes are terminal. The (py)(ph)CO molecule behaves as a N,O-bidentate (1.11) ligand in **1** and **3**. A terminal EtOH ligand completes the coordination sphere of In^{III} in **1**. The alkoxo oxygen atoms of the two 2.21 $(py)(ph)CH(O)^-$ ligands doubly bridge the In^{III} centers in **4** creating a $\{In^{III}_2(\mu\text{-}OR)_2\}^{4+}$ core; a nitrogen atom of one reduced organic ligand, two bromo ions and one terminal EtOH molecule complete the 6-coordination at each metal centre. Complexes **1**, **3** and **4** were characterised by IR and Raman spectroscopies, and the data were discussed in terms of their known solid-state structures. Molar conductivity data and ^1H NMR spectra were used in an attempt to probe the behaviour of the complexes in DMSO. The to-date observed metal ion-assisted/promoted transformations of (py)(ph)CO are also discussed.

Received 31st August 2022,
Accepted 27th September 2022

DOI: 10.1039/d2dt02851d

rsc.li/dalton

Open Access Article. Published on 28 2022. Downloaded on 5.11.2024 . 13:44:01.
This article is licensed under a Creative Commons Attribution 3.0 Unported Licence.

Introduction

The renaissance of inorganic chemistry in the early 1960s was a consequence of the discovery and study of transition-metal organometallic chemistry. The great advantage of organometallic chemistry is the ability of scientists to isolate and subsequently utilise unusual organic fragments bonded to a transition metal ion. In the last 30 years or so, alternative methods to ligand reactivity have been developed that involve classical coordination complexes (*i.e.* of Werner type) as opposed to organometallic compounds. The stimulus for such research activities came from the study of natural biological systems. It is well known that several types of enzymes bind or require metal ions to perform their roles. Since enzymes can utilise metal ions to perform complicated organic reactions under aerobic conditions in aqueous environments at room temperature and ambient pressure, it was logical for scientists to think that such reactions can be carried out on the bench, providing, for example, a better approach to homogeneous catalysis. Today there are many and varied "organic" reactions that proceed in the presence of metal ions, the latter promoting,

[a]*Department of Chemistry, University of Patras, 26504 Patras, Greece. E-mail: dapapaio@upatras.gr, perlepes@upatras.gr*
[b]*Institute of Chemical Engineering Sciences (ICE-HT), Foundation for Research and Technology-Hellas (FORTH), P.O. Box 1414, Platani, 26504 Patras, Greece*
[c]*NMR Facility, Instrumental Analysis Laboratory, School of Natural Sciences, University of Patras, 26504 Patras, Greece*
[d]*Centre de Recherche Paul Pascal, UMR 5031, CNRS, University of Bordeaux, 33600 Pessac, France. E-mail: pierre.dechambenoit@u-bordeaux.fr*

†Electronic supplementary information (ESI) available: Crystallographic data (Table S1–S4) and various structural plots of complexes **1**, **3** and **4**, and spectroscopic (IR, Raman, ^1H and ^{13}C NMR, ESI-MS, fluorescence) material for the compounds. CCDC 2203979–2203981. For ESI and crystallographic data in CIF or other electronic format see DOI: https://doi.org/10.1039/d2dt02851d

Open Access Article. Published on 28 2022. Downloaded on 5.11.2024 . 13:44:01.
This article is licensed under a Creative Commons Attribution 3.0 Unported Licence.

catalysing or initiating the reactions. Thus, metal ion-directed chemistry and the use of metal ions to control the stereochemical course of reactions are a "hot" research theme in contemporary inorganic chemistry.[1–7]

The principle of the reactivity of coordinated ligands is simple. Any chemical reaction involves movement of electrons (either complete transfer or sharing). Thus, anything that changes the distribution, movement or availability of electrons can affect the reactivity. When the coordination bond forms, the electronic arrangement in parts of the ligand is perturbed to some extent. Given the fact that the reactivity is based upon the electronic structure, it is obvious that the reactivity of coordinated ligands is different from that of the free ligands. The mechanisms with which a metal ion may alter the chemical behaviour of a coordinated ligand involve conformational, polarisation and π-bonding changes.[1]

Several reactions of carbonyl compounds, which are often significant in C–C bond formation, display sensitivity upon complexation with metal ions.[7] The coordination of a carbonyl molecule to a metal ion through the oxygen atom is expected to modify the reactivity of the carbonyl group. The commonest type of reaction associated with carbonyl compounds involves attack of the carbonyl carbon atom by a nucleophile. Since both the carbonyl carbon atom and the metal ion normally have electrophilic character, a nucleophile could initially attack at either the carbon atom of the carbonyl group or at the metal ion. This means that the products of the reaction can arise either by direct attack at the carbon by the free nucleophile or by attack at the metal centre followed by attack at carbon by the coordinated nucleophilic agent. There has been a debate about the predominant mechanism, *i.e.* attack by a free or by a coordinated nucleophile.[1,8,9]

In the last 25 years our groups have had an intense interest in the area of the reactivity of carbonyl-containing coordinated ligands of the general types A-CO-A,[10,11] A-CO-CO-A,[10,12] A-CO-A-CO-A,[12] where A is a donor group. We have concentrated mainly on di-2-pyridyl ketone, $(py)_2CO$, and discovered more than ten metal ion-assisted transformations.[10,13] Due to the polarisation effect, the already existing electrophilicity of the C=O carbon is increased dramatically by coordination of the oxygen atom in solution. The active character of the carbonyl group is further enhanced by the strong electron-attractive property of the 2-pyridyl rings. Thus, upon coordination to a metal centre, several nucleophiles can attack the carbonyl carbon (Scheme 1) leading to exciting coordinated ligands which in most cases can not been stabilized in the absence of metal ions. Single deprotonation of the ligands (deprotonation may be double in the case of H_2O as nucleophile), combined with the presence of donor atom(s) in the negatively charged nucleophile give a flexible character in the ligand with variable coordination modes, leading to coordination clusters and polymers with aesthetically beautiful structures and interesting properties (magnetic, optical, ...).

Based on the experience gained from our research efforts with $(py)_2CO$, we started to study the metal ion-involving chemistry of (py)CO(B), where B is a non-donor group. We

Scheme 1 General reactivity pattern of coordinated di-2-pyridyl ketone, $(py)_2CO$. The neutral nucleophile is represented by nucH and can be H_2O, alcohols, Me_2CO, MeCN, pyrazoles, secondary amino acids, *etc*. The attack of the nucleophile on the carbonyl carbon atom requires its deprotonation, which is often achieved by an external base. M^{n+} is the metal ion (n = 2, 3). When nucH is H_2O, the product is the *gem*-diol derivative of $(py)_2CO$, $(py)_2C(OH)_2$, whereas the addition of alcohols (ROH) produces the hemiacetal form of $(py)_2CO$, $(py)_2C(OR)(OH)$. Note that compounds $(py)_2C(nuc)(OH)$ and their anionic forms do not exist as free species, but only in the presence of metal ions (*i.e.* as ligands in their respective metal complexes). Important note: in the abbreviations of the ligands, the carbonyl oxygen atom is written without parenthesis, whereas the oxygen atoms which form single bonds with the central carbon are written within parenthesis.

were interested in investigating if the latter ligands could undergo metal ion-assisted reactivity on the carbonyl group; if yes, we anticipated different identities of the products and possibly new reactivity pathways. This work describes some aspects of In(III)/(py)(ph)CO chemistry with emphasis on the reactivity characteristics of its carbonyl group; (py)(ph)CO is 2-benzoylpyridine (Scheme 2), which normally behaves as a N(ring), O(carbonyl)-chelating ligands.[14] This ligand does not possess the second ring-N atom that is present in $(py)_2CO$. The two ligands have the same size, while the phenyl group has also an electron-withdrawing character (albeit weaker than that of the 2-pyridyl group). In addition, both ligands lack acidic α-hydrogens (*i.e.* C–H bonds adjacent to the carbonyl group), present, for example, in 2-acetylpyridine where the C–H bonds of the methyl group are polar and potential reaction sites. The rather little investigated reactivity of (py)(ph)CO towards transition metal ions (Ni^{II}, Cu^{I}, Cu^{II}, Ru^{II}, Re^{V}) has been studied (*vide infra*) by few groups[15] – including our group[16] – with impressive results; the general conclusion of those studies is that there is space for further research in this area. This belief was the main stimulus of the present report.

Contrary to previous work which involved 3d-, 4d- and 5d-metals,[15,16] we selected to work with the group 13 In(III) ion.

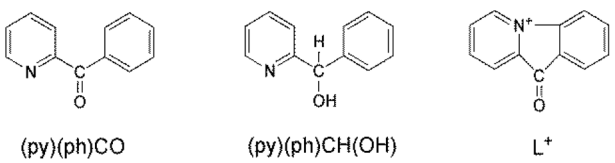

Scheme 2 The free 2-benzoylpyridine ligand, (py)(ph)CO, whose In(III) chemistry has been studied in the present work, its reduced analogue (pyridin-2-yl)methanol, (py)(ph)CH(OH), and the 9-oxo-indolo[1,2-*a*] pyridinium cation (L^+); all these species are discussed in the text. The important note mentioned in the caption of Scheme 1 is valid also for L^+ and the ligands illustrated in the schemes that follow.

This journal is © The Royal Society of Chemistry 2022

Open Access Article. Published on 28 2022. Downloaded on 5.11.2024 . 13:44:01.
This article is licensed under a Creative Commons Attribution 3.0 Unported Licence.

The main reason of our choice was the recently reported unusual reactivity of $(py)_2CO$ towards this metal ion.[17] In addition to the well established importance of indium in various aspects of material science (*e.g.* development of LCD monitors and television sets,[18a] applications of indium-tin oxide thin films,[18b] perovskites,[18c,d] optical materials,[18e] ...), In (III) coordination complexes continue to attract the interest of many inorganic chemistry groups around the world due to their involvement in MOF chemistry (*e.g.* as sensors[19a] and efficient photocatalysts for hydrogen evolution[19b]), homogeneous (*e.g.* ring-opening polymerization of cyclic ethers[19c]) and heterogeneous (*e.g.* cycloaddition of CO_2 with epoxides[19d]) catalysis, medicinal chemistry,[19g] NMR spectroscopy (^{115}In with 95.7% natural abundance and nuclear spin 9/2 is a valuable NMR-active nucleus in solid-state research[17,19h]) and synthetic inorganic chemistry.[19i,j]

Experimental section

Chemicals and instrumentation

All manipulations were performed in the normal laboratory atmosphere under aerobic conditions. The materials (reagent grade) and solvents were used as received. Phenyl(pyridin-2-yl) methanol [an alternative name is (2-pyridine)(phenyl)methanol] (Scheme 2), (py)(ph)CH(OH), was synthesized by the reduction of (py)(ph)CO with $NaBH_4$ as previously reported;[20] its purity was checked by microanalyses, IR and ^{1}H NMR spectra. Elemental microanalyses (C, H, N) were performed by the University of Patras Instrumental Analysis Laboratory. Melting points were determined with an electrothermal apparatus and are uncorrected. Conductivity measurements were performed in DMSO at 25 ± 1 °C with a Metrohm-Herisau E-527 bridge and a cell of standard constant; the concentration of the solutions was ~10^{-3} M. IR spectra were recorded using a PerkinElmer 16 PC FT-IR spectrometer. For the Raman measurements, the T64000 Horiba-Jobin Yvon micro-Raman setup was used. The excitation wavelength was 514.5 nm emitted from a DPSS laser (Cobolt Fandango TMISO laser, Norfolk, UK). The laser power on the samples was 2 mW. The backscattered radiation was collected from a single configuration of the monochromator after passing through an appropriate edge filter (LP02-633RU-25, laser2000, UK, Ltd, Huntingdon, Cambridgeshire, UK). The calibration of the instrument was achieved *via* the standard Raman peak position of Si at 520.5 cm^{-1}. The spectral resolution was 5 cm^{-1}. An attempt to obtain the Raman scattering of $[In_2Br_4\{(py)(ph)CH(O)\}_2(EtOH)_2]$ (*vide infra*) was also made. However, it was not possible to record the Raman spectrum since fluorescence of the samples was detected, overlapping the Raman effect. With the goal to bypass the fluorescence of the compound, we used a different wavelength (632.8 nm) of the Raman excitation laser line for the measurements; our attempts to overcome the fluorescence effect were again unsuccessful. The inherent fluorescence of the sample has been further supported through photoluminescence measurements (Fig. S1†). ^{1}H and ^{13}C NMR spectra were obtained at 600 and 150 MHz, respectively, on a Bruker Avance III HD spectrometer; the signal of the undeuterated portion of the solvent (d_6-DMSO) was used as reference. Electron-spray ionization (ESI) mass spectra were recorded at 30 eV on a Waters Micromass ZQ spectrometer using HPLC grade MeOH as solvent, in the positive and negative modes.

Synthetic procedures

Preparation of $[InCl_3\{(py)(ph)CO\}(EtOH)]\cdot\{(py)(ph)CO\}$ (1) and $\{(pyH)(ph)CO\}Cl$ (2) in a mixture. To a solution of (py)(ph)CO (0.73 g, 0.40 mmol) in EtOH (2 mL) was added dropwise a solution of $InCl_3\cdot4H_2O$ (0.059 g, 0.20 mmol) in the same solvent (3 mL). The colourless reaction solution was stirred for 20 min, filtered and stored at 5 °C. X-ray quality colourless crystals of **1** and dark yellow crystals (not suitable for single-crystal X-ray crystallography) of **2** were obtained in a period of 2–3 d. The colour of the solution became slowly yellow during the crystallisation period. The crystals were collected by filtration, separated manually, washed with Et_2O (2 × 2 mL) and dried in air. Typical yields were in the ranges 65% (based on the metal available) for **1** and 10% (based on the ligand available) for **2**. Analytical data for **1**, calcd for $C_{26}H_{24}InN_2O_3Cl_3$ (found values are in parentheses): C 49.28 (48.93), H 3.83 (3.88), N 4.42 (4.54)%. Λ_M (DMSO, 10^{-3} M, 25 °C) = 3 S cm^2 mol^{-1}. IR bands (KBr, cm^{-1}): 3443wb, 3088w, 3057w, 2974w, 1668s, 1624s, 1590s, 1566sh, 1466w, 1442m, 1386w, 1329s, 1279w, 1257m, 1170w, 1093w, 1017m, 949m, 882w, 850w, 819w, 776m, 753w, 731w, 702s, 649m, 573w, 483w, 453w, 426w. Selected Raman peaks (cm^{-1}): 1671m, 1626s, 1595m, 1570s, 1474m, 1322m, 1179m, 1112w, 1053w, 1022m, 1000s, 733m, 618w, 572w, 309m, 233w, 162m. ^{1}H NMR (d_6-DMSO, δ/ppm): 8.73 (d, 2H), 8.08 (td, 2H), 7.98 (mt, 6H), 7.68 (mt, 4H), 7.54 (t, 4H), 4.36 (sb, 1H), 3.45 (q, 2H), 1.07 (t, 3H). Analytical data for **2**, calcd for $C_{12}H_{10}NOCl$ (found values are in parentheses): C 65.60 (65.19), H 4.60 (4.72), N 6.38 (6.23)%. Λ_M (DMSO, 10^{-3} M, 25 °C) = 38 S cm^2 mol^{-1}. The $AgNO_3$ test of a sample of the compound in 2 N HNO_3 was positive for Cl^- ions. M.p. 168 °C. IR bands (KBr, cm^{-1}): 3065w, 2924w, 2856wb, 1738s, 1626s, 1590m, 1567w, 1493w, 1451m, 1359sh, 1328s, 1259m, 1221w, 1167m, 1107m, 1016m, 956m, 914m, 811m, 754s, 699s, 649s, 565mb, 438w. ^{1}H NMR (d_6-DMSO, δ/ppm): 8.72 (mt, 1H), 8.49 (d, J = 8.8 Hz, 1H), 8.08 (td, J = 8.1 and 1.8 Hz, 1H), 7.99 (dt, J = 7.8 and 0.6 Hz, 1H), 7.98–7.95 (mt, 2H), 7.70–7.65 (mt, 2H), 7.55 (t, J = 7.8 Hz, 2H). ^{13}C {^{1}H} NMR (d_6-DMSO, δ/ppm): 194.6, 154.5, 149.0, 138.2, 136.1, 133.7, 130.8 (2C), 128.7 (2C), 127.3, 124.6. MS-ESI (m/z): 184.56 $[(py)(ph)CO + H]^+$, 183.70 $[(py)(ph)CO]^+$, 182.37 $[(py)(ph)CO\text{-}H]^+$, 106.71 $[(ph)CHO]^+$, and 259.22, 257.23 and 255.23 $[(py)(ph)CO + 2HCl]^-$.

Preparation of $[InCl_3\{(py)(ph)CO\}(EtOH)]\cdot\{(py)(ph)CO\}$ (1) free from the side product 2. To a solution of (py)(ph)CO (0.73 g, 0.40 mmol) in EtOH (4 mL) was added dropwise a solution of $InCl_3\cdot4H_2O$ (0.059 g, 0.20 mmol) in the same solvent (5 mL). The colourless reaction solution was stirred for 20 min, filtered and stored at 5 °C. Few single crystals of col-

Open Access Article. Published on 28 2022. Downloaded on 5.11.2024 . 13:44:01.
This article is licensed under a Creative Commons Attribution 3.0 Unported Licence.

ourless **1** appeared within 12 h. The solution remained colourless during this short crystallisation period. The crystallisation stopped at this point and the crystals were collected by filtration, washed with Et_2O (2 × 1 mL) and dried in air. Close inspection of the collected material did not reveal any signs of the yellow crystals of **2** (*vide supra*). Typical yields were ∼20% (based on the metal available). Analytical data, calcd for $C_{26}H_{24}InN_2O_3Cl_3$ (found values are in parentheses): C 49.28 (49.53), H 3.83 (3.71), N 4.42 (4.39)%. The IR, Raman and solution ^{1}H NMR spectra of the powdered crystals were identical with those of the authentic material (isolated in a mixture with **2**, *vide supra*) whose identity was proven by solution of its structure.

Preparation of (L)[$InBr_4${(py)(ph)CO}] (3) and [In_2Br_4{(py)(ph)CH(O)}$_2$ $(EtOH)_2$] (4) in a mixture, where L^+ is the 9-oxo-indolo [1,2-α] pyridinium cation (Scheme 2). To a solution of (py)(ph)CO (0.73 g, 0.40 mmol) in EtOH (2 mL) was added dropwise a solution of $InBr_3$ (0.071 g, 0.20 mmol) in the same solvent (3 mL). The colourless reaction solution was stirred for 20 min during which time a colour change to pale yellow was noticed, filtered and stored in a closed flask at room temperature. X-ray quality yellow crystals of **3** and colourless crystals of **4** were obtained in a period of ∼15 d. The colour of the solution became slowly darker yellow during the crystallisation period. The crystals were collected by filtration, separated manually, dried in air and characterized independently. Typical yields were ∼30% for **4** and ∼40% for **3** (both based on the total amount of indium available). Analytical data for **3**, calcd for $C_{24}H_{17}InN_2O_2Br_4$ (found values are in parentheses): C 36.04 (36.14), H 2.15 (2.20), N 3.50 (3.41)%. Λ_M (DMSO, 10^{-3} M, 25 °C) = 36 S cm^2 mol^{-1}. IR bands (KBr, cm^{-1}): 3086w, 3054w, 2972w, 1668s, 1622m, 1589m, 1566sh, 1468w, 1440m, 1383m, 1329s, 1256s, 1169m, 1091m, 1054w, 1018s, 948m, 879w, 817m, 775m, 751m, 730w, 701s, 648m, 527w, 481w, 450w, 428m. Selected Raman peaks (cm^{-1}): 1670m, 1628s, 1594s, 1569s, 1474w, 1322wb, 1179m, 1019m, 1000m, 729w, 572w, 196m, 153w. ^{1}H NMR (d_6-DMSO, δ/ppm): 8.73 (d, 2H), 8.08 (mt, 2H), 8.01–7.95 (mt, 5H), 7.68 (mt, 4H), 7.55 (t, 4H). Analytical data for **4**, calcd for $C_{28}H_{32}In_2N_2O_4Br_4$ (found values are in parentheses): C 33.30 (33.51), H 3.20 (3.09), N 2.77 (2.65)%. Λ_M (DMSO, 10^{-3} M, 25 °C) = 7 S cm^2 mol^{-1}. IR bands (KBr, cm^{-1}): 3313mb, 3029w, 2978w, 1608m, 1570w, 1482m, 1455w, 1439m, 1404w, 1290m, 1262w, 1211m, 1158w, 1082m, 1064s, 1047s, 1028s, 924w, 876m, 762s, 737w, 702m, 684sh, 651m, 623m, 520m, 464w, 415w. No satisfactory Raman spectrum for **4** could be obtained (see "Chemicals and instrumentation" above). ^{1}H NMR (d_6-DMSO, δ/ppm): 8.72 (d, 2H), 8.07 (td, 2H), 7.98 (mt, 6H), 7.67 (mt, 4H), 7.54 (t, 4H), 4.35 (sb, 2H), 3.47 (q, 4H), 1.06 (t, 6H).

Preparation of [In_2Br_4{(py)(ph)CH(O)}$_2$$(EtOH)_2$] (4) free from 3. The same procedure as described above for the isolation of **3** and **4** in a mixture was followed, the only difference being the volume of EtOH which was 8 mL (instead of 5). Upon storage of the yellow reaction solution in a closed flask at room temperature for a period of 2 months, only the colourless crystals of **4** were observed from a dark yellow solution; the yellow crystals of **3** had been redissolved. The crystals were collected by filtration, washed with Et_2O (2 × 1 mL) and dried in air. The yield was ∼25%. Analytical data, calcd for $C_{28}H_{32}In_2N_2O_4Br_4$ (found values are in parentheses): C 33.70 (34.01), H 3.20 (3.12), N 2.77 (2.60)%. The IR and solution ^{1}H NMR spectra of the powdered crystals were identical with those of the authentic material (isolated in a mixture with **3**, *vide supra*) whose identity was proven by solution of its structure.

Preparation of [In_2Br_4{(py)(ph)C(H)(O)}$_2$$(EtOH)_2$] (4) from the reaction of (py)(ph)CH(OH) and $InBr_3$. A solution of $InBr_3$ (0.071 g, 0.20 mmol) in EtOH (3 mL) was added to a solution of (py)(ph)CH(OH)[15] (0.046 g, 0.25 mmol) in the same solvent (2 mL). The reaction solution was stirred overnight, during which time a white microcrystalline powder was precipitate. This was collected by filtration, washed with Et_2O (2 × 2 mL) and dried in air. The yield was ∼70%. Analytical data, calcd for $C_{28}H_{32}In_2N_2O_4Br_4$ (found values are in parentheses): C 33.30 (39.71), H 3.20 (3.16), N 2.77 (2.70)%. The IR spectrum of the powder was identical with that of the authentic material, whose structure was determined by single-crystal X-ray crystallography.

Single-crystal X-ray crystallography

Crystallographic data (Table S1†) were collected with a Bruker APEX II Quasar diffractometer, equipped with a graphite monochromator centred on the path of Mo Kα radiations. Single crystals of **1**, **3** and **4**, taken directly from the reaction solution, were coated with Cargille™ NHV immersion oil and mounted on a fiber loop, followed by data collection at 120 K. The program SAINT was used to intergrate the data, which were thereafter corrected using SADABS.[21] The structures were solved using SHELXT[22a] and refined by full-matrix least-squares technique on F^2 using SHELXL-2018.[22b] All non-H atoms were refined with anisotropic displacement parameters, whereas H atoms were assigned to ideal positions and refined isotropically using a riding model, except those on the O atom of coordinated EtOH molecules in **1** and **4** which were located on the difference density map and introduced using DFIX constraints.

The crystals of **3** are very thin needles. The small size makes the diffraction very poor, and the anisotropic shape makes the diffraction strongly dependent on the orientation of the crystal. Therefore, the data were cut at 1.05 Å as there is no diffraction above and R_{int} becomes larger. The result is a low θ_{max} value, as well as a poor resolution and data/parameters ratio. SIMU restraints were applied to prevent nearly 2D thermal ellipsoids, as a probable consequence of the low resolution.

Crystallographic data for the structures reported in this paper have been deposited with the Cambridge Crystallographic Data Centre as supplementary publication with the deposition numbers 2203979–2203981.†

Results and discussion

Synthetic comments

Our approach to activate the proligand (py)(ph)CO by indium (III) for further reactivity was to treat $InX_3{\cdot}nH_2O$ (X = Cl, n = 3; X

 This journal is © The Royal Society of Chemistry 2022

Open Access Article. Published on 28 2022. Downloaded on 5.11.2024 . 13:44:01.
This article is licensed under a Creative Commons Attribution 3.0 Unported Licence.

= Br, n = 0) with the ligand in the absence of external base (addition of Et_3N or NaOMe resulted in amorphous solids which could not be characterized). At the outset of our efforts we realized that the $InX_3{\cdot}nH_2O$/(py)(ph)CO reaction systems are complicated, and the reactivity patterns of the chloride and bromide "salts" are completely different. For this reason, we kept as many as possible synthetic (reaction time and temperature, molar ratio of the reactants, solvent, concentrations in some experiments) and crystallization (storage of the reaction solutions at room temperature or 5 °C) parameters constant for comparable results. The discussion that follows represents simplified mechanisms, and it is supported by X-ray structural studies and strong spectroscopic evidence of the main products (**1**, **3**, **4**) and the side product (**2**), see the next two parts of this section ("Description of structures" and "Spectroscopic discussion in brief"). Treatment of $InCl_3{\cdot}4H_2O$ with (py)(ph)CO (1 : 2) in EtOH at room temperature gave a colourless solution which became slowly yellow upon storage at 5 °C for a period of 2–3 days; from this solution was isolated a mixture of colourless and dark yellow crystals of [$InCl_3${(py)(ph)CO}(EtOH)]·{(py)(ph)CO} (**1**; yield ~65%) and {(pyH)(ph)CO}Cl (*i.e.* the hydrochloride salt of 2-benzoylpyridine, **2**; yield <15%), respectively. Due to the sharp colour and shape difference, the crystals were separated manually and independently characterised by microanalyses, IR, Raman and NMR spectra; in addition, the structure of **1** was unambiguously determined by single-crystal X-ray crystallography, while the identity of **2** was further supported by ESI-MS spectra. The dark yellow compound is clearly a byproduct of the reaction since its yield never exceeded 15%. Since the reaction solution remains colourless during the first hours of the crystallisation, we suspected that there is a kinetic effect in the formation of **1** and **2** in solution. Thus, we stopped the crystallisation after 12 h and collected the precipitated crystals of pure **1** from an almost colourless solution. To avoid coprecipitation of **2**, we used a more dilute reaction solution (compared with the solution that gave the mixture) because we had observed that **2** is more soluble in EtOH than **1**. A consequence of these two modifications is the low yield for the isolation of pure **1**.

A possible mechanistic scheme accounting for the formation of **1** and **2** is shown in Scheme 3. According to this scheme, (py)(ph)CO initially forms the chelate **I**. Due to steric or/and electronic reasons, a second chelating ligand cannot be coordinated to In^{III} to yield the anticipated 6-coordinate complex. Instead, the much less sterically demanding solvent molecule is coordinated to the metal ion increasing the coordination number of In^{III} from five to six. This complexation leads to increased acidity of the ethanol hydroxyl proton which is then associated to the N atom of a second (py)(ph)CO molecule through an intermolecular H bond giving rise to the crystalline complex **1**. On standing at ambient temperature in solution, complex **1** is slowly converted to another crystalline compound which precipitates out of the reaction mixture, and proved by a combination of spectroscopic techniques to be {(pyH)(ph)CO}Cl (**2**); the formation of the latter salt involves the base-induced decomposition of the initial complex **1** with

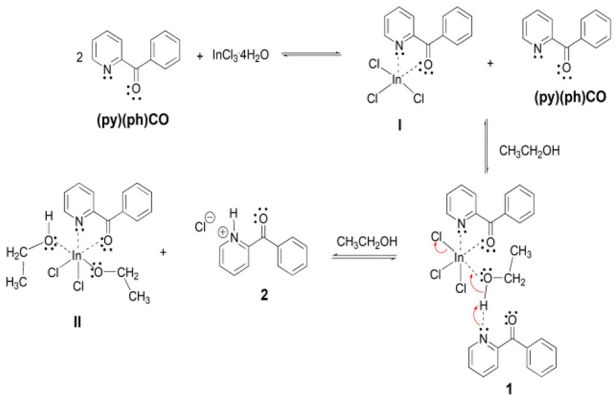

Scheme 3 The proposed mechanism for the formation of complex [$InCl_3${(py)(ph)CO}(EtOH)]·{(py)(ph)CO} (**1**) and 2-benzoylpyridinium chloride, {(pyH)(ph)CO}Cl (**2**).

formation of the new species **II** (or a dimer of it formed through bridging of the deprotonated ethoxido groups) which is obviously soluble in EtOH. The precipitation of the salt **2** from an ethanol solution might be attributed to a strong intramolecular N–H···$O_{carbonyl}$ H bond forming a five-membered ring, which increases the hydrophobicity of the hydrochloride salt.

The $InBr_3$/(py)(ph)CO reaction pattern is completely different. Treatment of $InBr_3$ with (py)(ph)CO (1 : 2) in EtOH at room temperature gave a colourless solution which rapidly turned to yellow upon stirring. Storage of the reaction solution at room temperature for ~15 days resulted in the precipitation of a mixture of yellow crystals of (L)[$InBr_4${(py)(ph)CO}] (**3**; yield ~40%) and colourless crystals of [In_2Br_4{(py)(ph)CH(O)}$_2$(EtOH)$_2$] (**4**; yield ~30%), where L^+ is the cation shown in Scheme 2 and (py)(ph)$CH(O)^-$ is the monoanion of the reduced form of 2-benzoylpyridine whose structural formula (in the form of the neutral molecule) is also shown in Scheme 2. Due to the colour and shape difference, the crystals were separated manually and their solid-state structures were solved by single-crystal X-ray crystallography; they were also characterised by spectroscopic methods and microanalyses. Since we noticed that the amount of the yellow crystals decreased as a function of crystallisation time, probably due to their dissolution in EtOH (an indication of this is the color change of the supernatant solution to more intense, *i.e.* dark yellow, with time), we devised a method to isolate pure **4**. The same procedure was followed, but with two modifications. The reaction solution was more dilute (to facilitate dissolution of **3**) and the crystallisation period increased to ~2 months; these modifications lead to the isolation of pure **4** (albeit with a low yield) from a dark yellow reaction mixture. The formation of **3** and **4**, that contain L^+ and the ligand (py)(ph)$CH(O)^-$, using the above mentioned procedures, is clearly In^{III}-promoted/assisted. "Blind" experiments, *i.e.* without addition of $InBr_3$, under identical conditions resulted in the isolation of pure (ph)(ph)CO (microanalyses, IR and ^{1}H NMR evidences) after slow evaporation of EtOH at room temperature. As anticipated,

Open Access Article. Published on 28 2022. Downloaded on 5.11.2024 . 13:44:01.
This article is licensed under a Creative Commons Attribution 3.0 Unported Licence.

pure **4** can also be prepared by the 1 : 1 reaction between $InBr_3$ and performed[20] (py)(ph)CH(OH) in a good yield (~70%). Although we performed more than 300 reactions changing several reaction and crystallisation conditions, we have not been able to prepare **3** in pure form.

A possible mechanistic scheme accounting for the formation of **3** and **4** is shown in Scheme 4. According to this proposal, (py)(ph)CO initially forms the chelate **III**, similar to the one formed with $InCl_3$ (**I** in Scheme 3). This molecule takes up a second (py)(ph)CO ligand which is coordinated in a monodentate manner through its carbonyl oxygen atom, forming the intermediate **IV**. Then a nucleophilic aromatic substitution with ring closure takes place through an intramolecular nucleophilic attack (a Michael-type reaction) of the uncoordinated pyridyl nitrogen atom on the adjacent phenyl ring, which is facilitated by the conjugated carbonyl group being activated through coordination to In^{III}. The thus obtained enolate intermediate **V** re-establishes the carbonyl functionality with concomitant rearomatization of the phenyl ring and simultaneous expulsion of a hydride (H^-) ion, which is used to reduce the carbonyl group of the other (*i.e.* coordinated) (py)(ph)CO molecule. That way two new intermediates are formed, namely the coordinatively unsaturated new complex **VI** and the cyclized ammonium-type salt $(L)^+Br^-$. Finally, the initial chelate **III** is combined with the salt $(L)^+Br^-$ providing the product $(L)[InBr_4\{(py)(ph)CO\}]$ (**3**). On the other hand, the intermediate complex **VI** (in which the coordination number of In^{III} is four) dimerizes and is further associated with two solvent (EtOH) molecules to form the other product **4** which has the normal coordination number six at each In^{III} centre.

Compounds **1** and **4** are slightly soluble in EtOH, whereas **2** and **3** have a moderate solubility. All compounds are readily soluble in DMF and DMSO, but the solid-state structures of **1**, **3** and **4** are not retained (at least in DMSO) as proven by ^1H NMR spectroscopy (*vide infra*). Compound **2** has a limited solubility in H_2O, whereas complexes **1**, **3** and **4** are not stable as evidenced by the IR spectra of the collected solid materials.

As mentioned in Introduction, the reactivity of coordinated (py)(ph)CO has been investigated by few groups,[15] including our group.[16] The ligation modes of the resulting ligands are shown in Scheme 5, which also includes the structural formula of the cation L^+ which counterbalances the charges of the anionic polymers $\{[Cu^IX_2]\}_n^{n-}$ (X = I, SCN)[15a,b] and $[InBr_4\{(py)(ph)CO\}]^-$ in complex **3**; a mechanism of its formation is proposed in this work (Scheme 4). In complex $[Ru^{II}Cl\{(py)CO_2\}(CO)(PPh_3)_2]$,[15c] the ligand has been oxidized to the coordinated picolinate(−) ion. Complexes $[Re^VOX_2\{(py)(ph)CH(O)\}(PPh_3)]$ (X = Cl, Br),[15d,g] $[Sn^{II}(L')\{(py)(ph)CH(O)\}]$,[15h] where $(L')^-$ is $HC\{CMeN(2,6\text{-}^iPr_2C_6H_3)_2\}^-$, and $[In_2Br_4\{(py)(ph)CH(O)\}_2(EtOH)_2]$ (**4**) contain the anionic ligand (py)(ph)CH

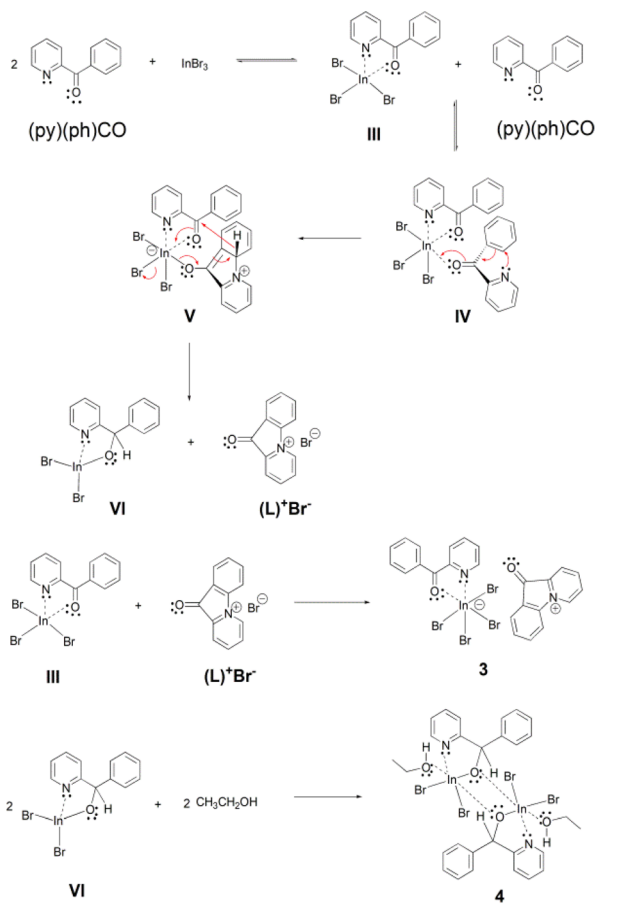

Scheme 4 The proposed mechanism for the formation of complexes $(L)[InBr_4\{(py)(ph)CO\}_2]$ (**3**) and $[In_2Br_4\{(py)(ph)CH(O)\}_2(EtOH)_2]$ (**4**).

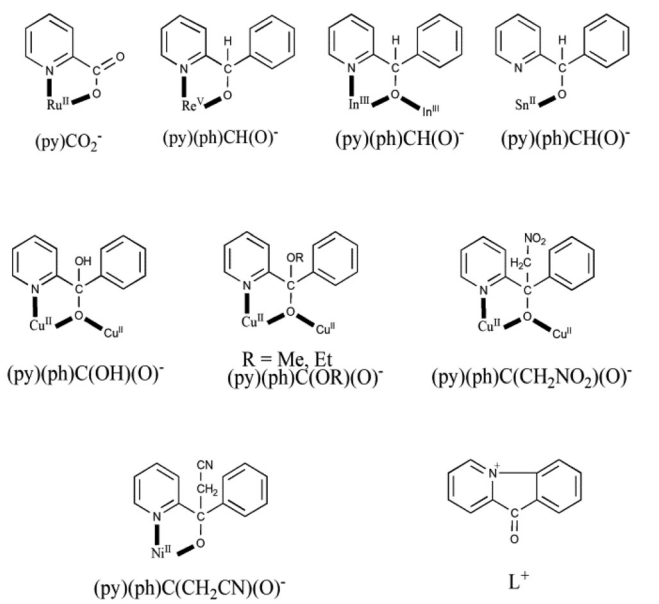

Scheme 5 Structural formulae, abbreviations and crystallographically established coordination modes of ligands derived from the to-date metal ion-assisted reactivity of (py)(ph)CO. The bridging behaviour of $(py)(ph)CH(O)^-$ from such reactivity studies has been observed for the first time in $[In_2Br_4\{(py)(ph)CH(O)\}_2(EtOH)_2]$ (**4**). The cation L^+ has also resulted from (py)(ph)CO and it behaves as counterion in anionic polymers of Cu(I) and in complex $(L)[InBr_4\{(py)(ph)CO\}]$ (**3**), also described in this work. A list of the relevant complexes appears in Table 1.

This journal is © The Royal Society of Chemistry 2022

Open Access Article. Published on 28 2022. Downloaded on 5.11.2024 . 13:44:01.
This article is licensed under a Creative Commons Attribution 3.0 Unported Licence.

$(O)^-$ which is the 2-electron reduced form of (py)(ph)CO. Complexes $[Cu_2^{II}\{(py)(ph)C(OH)(O)\}_2\{(py)(ph)CO\}_2(H_2O)](ClO_4)_2$,[15e,f] $[Cu_2^{II}\{(py)(ph)C(OMe)(O)\}_2\{(py)(ph)CO\}_2](ClO_4)_2$,[16a] $[Cu_4^{II}(OMe)_2(NO_3)_4\{(py)(ph)C(OMe)(O)\}_2\{(py)(ph)CO\}_2]$[16a] and $[Cu_2^{II}(NO_3)_2\{(py)(ph)C(OEt)(O)\}_2(EtOH)]$[16a] contain the bridging monoanion of the *gem*-diol (the first one) and the hemiacetal (the next three ones) forms of (py)(ph)CO, formed *in situ* by the nucleophilic addition of H_2O and alcohols (MeOH, EtOH) on the electrophilically activated (through coordination of the carbonyl oxygen atom and possibly the pyridyl ring) carbonyl carbon atom and subsequent deprotonation. For the formation of complexes $[Cu_2^{II}(NO_3)_2\{(py)(ph)C(CH_2NO_2)(O)\}_2]$[16a] and $[Ni^{II}\{(py)(ph)C(CH_2CN)(O)\}_2]$,[16b] which were prepared under strongly basic conditions, the OH^- ion abstracts one of the methyl hydrogens of the solvent (CH_3NO_2, CH_3CN); once the carbanion ($^-CH_2NO_2$, $^-CH_2C{\equiv}N$) is formed, it attacks the positive ($\delta+$) carbonyl carbon atom of (py)(ph)CO. The metal ion polarises further the carbonyl group of (py)(ph)CO, making it more susceptible to nucleophilic attack by $^-CH_2NO_2$ or $^-CH_2CN$ and stabilises the final ligand.

Description of structures

Partially labelled molecular structures and the supramolecular networks of complexes **1**, **2** and **3** are shown in Fig. 1–4 and S2–S5.† Selected interatomic distances and angles are listed in Tables S2–S4.†

Complex **1** crystallises in the monoclinic space group $P2_1/c$. Its structure consists of mononuclear molecules $[InCl_3\{(py)(ph)CO\}(EtOH)]$ and lattice (py)(ph)CO molecules in an 1 : 1 ratio. In the complex molecule the In^{III} atom is 6-coordinate. The ligands are three terminal chloro (or chlorido) atoms (Cl1, Cl2, Cl3), one EtOH molecule and one bidentate chelating ($\eta^1{:}\eta^1$ or 1.11 adopting the Harris notation[23]) (py)(ph)CO molecule. The metal coordination geometry is distorted octahedral,

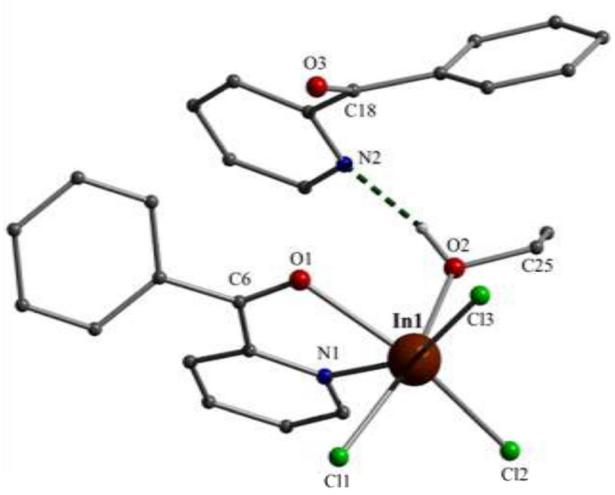

Fig. 1 Partially labelled plots of the structures of the molecules $[InCl_3\{(py)(ph)CO\}(EtOH)]$ and lattice (py)(ph)CO (upper part) that are present in complex **1**. The dark green dashed line indicates the intramolecular H bond.

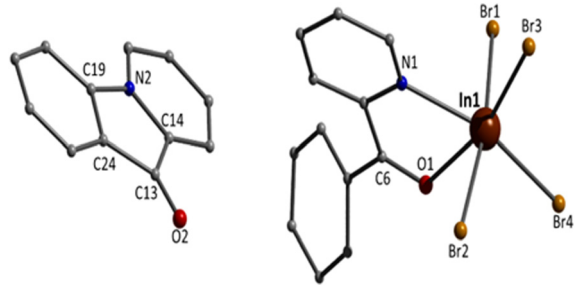

Fig. 2 Partially labelled plots of the structures of the anion $[InBr_4\{(py)(ph)CO\}]^-$ (right) and the cation L^+ (left) that are present in complex **3**. H atoms are omitted for clarity. Colour code: C, grey; N, blue; O, red; H, white; Br, orange; In, brown.

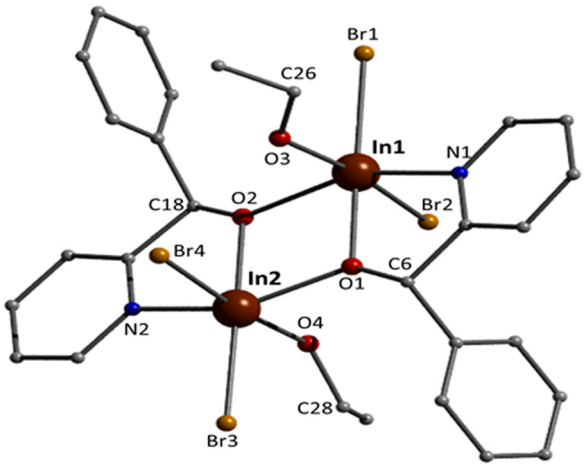

Fig. 3 Partially labelled plot of the structure of the molecule $[In_2Br_4\{(py)(ph)CH(O)\}_2(EtOH)_2]$ that is present in complex **4**. H atoms are omitted for clarity. Colour code: C, grey; N, blue; O, red; Br, orange; In, brown.

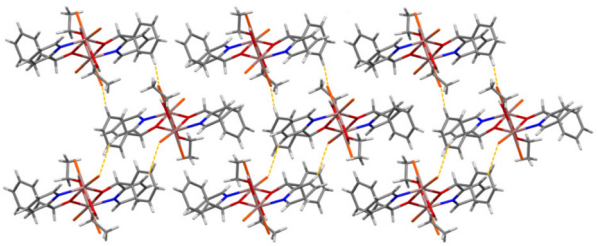

Fig. 4 Stick representation of the crystal structure of **4** along the (*ac*) plane, showing the packing of the dinuclear molecules and the weak $C_{aromatic}$–H···Br H-bonding interactions (dashed orange lines) that form an 1D network along the α crystallographic axis. Colour code: C, grey; N, blue; O, red; Br, orange; In, brown.

the *trans* angles being in the range 158.0(1)–166.0(1)°. The distortion is primarily a consequence of the small bite angle [69.0(1)°] of the bidentate ligand. The three chloro ligands occupy *cis* (or *fac*) positions in the octahedron. The In1–Cl, In1–O and In–N bond lengths are typical for complexes with octahedral

Open Access Article. Published on 28 2022. Downloaded on 5.11.2024 . 13:44:01.
This article is licensed under a Creative Commons Attribution 3.0 Unported Licence.

indium(II).[17,19d,24] The carbonyl C6–O1 bond of the coordinated (py)(ph)CO molecule is longer than that of the free (*i.e.* uncoordinated) molecule[25] [1.234(2) *vs.* 1.213(2) Å] due to coordination which weakens the carbonyl bond. This bond length is 1.217(2) Å in the lattice (ph)(ph)CO molecule of the compound, similar with that of the free one.[25] Another consequence of the formation of the chelating ring in **1** is the position of the pyridyl nitrogen and carbonyl group; these are on opposite sides in the free molecule[25] and on the same side in the coordinated (ph)(ph)CO.

The In(III) complex in **1** is H-bonded with the lattice (py)(ph)CO molecule through a O–H···N H bond involving the oxygen atom of the coordinated EtOH molecule (O2) as donor and the free pyridyl nitrogen atom (N2) as acceptor, the O···N distance being 2.675(4) Å. Weaker intermolecular C–H···O H bonds between the aromatic rings and the carbonyl groups are also present; together with $C_{aromatic}$–H···Cl H bonds, all these weak interactions form a 3D lattice in the crystal (Fig. S2†). Compound **1** is the first structurally characterized In(III) complex containing (ph)(ph)CO as ligand.

Although the quality of the crystal structure of **3** is not high, the basic structural features are clearly visible. The complex crystallises in the monoclinic space group *C*2/*c*. Its structure consists of mononuclear $[InBr_4\{(py)(ph)CO\}]^-$ anions and L^+ cations in an 1 : 1 ratio. In the anion, the 6-coordinate In^{III} atom is bonded to four bromo (or bromido) atoms and to one 1.11 (py)(ph)CO ligand. The In^{III}–Br bond lengths are in the narrow 2.563(2)–2.647(2) Å. Again the carbonyl bond of the coordinated (py)(ph)CO molecule is weaker than that of the free ligand[25] [1.251(19) *vs.* 1.213(2) Å] due to the coordination, but similar with the corresponding bond length of the coordinated (py)(ph)CO molecule in **1**. The metal coordination geometry is distorted octahedral, with the *trans* angles in the range 158.2(4)–169.8(1)°. The L^+ cation is planar the C13–O2 and C19–N2 bond distances are 1.18(2) and 1.41(2) Å, indicative of double carbon–oxygen and single carbon–nitrogen bonds, respectively, in agreement with its formulation (Scheme 2). The carbonyl bond length is similar with the corresponding bond distances in the free ligand[25] and in the lattice (py)(ph)CO molecule in **1**. This bond length is also close with that in the Cu(I) complexes that contain the L^+ cation (Table 1).

The supramolecular packing of the anions and cations in the crystal structure of **3** involve weak interionic $C_{aromatic}$–H···$O_{free\ carbonyl}$ and $C_{aromatic}$–H···Br H-bonding interactions, forming a 3D network in the crystal (Fig. S4†).

The L^+ cation is also present in the structures of the anionic polymers $\{(L)[Cu^I_2I_2]\}_n$ [15a] and $\{(L)[Cu^I(SCN)_2]\}_n$,[15b] which were isolated from CuI/(py)(ph)CO and Cu(SCN)/(py)(ph)CO reaction mixtures in EtOH, respectively.

Complex **4** crystallises in the monoclinic space group $P2_1/c$. Its structure contains dinuclear $[In_2Br_4\{(ph)(ph)CH(O)\}_2(EtOH)_2]$ molecules. The complex contains both enantiomeric forms of the (py)(ph)CH(O)$^-$ ligand, with *S* and *R* chiralities on C6 and C18, respectively, placing the phenyl rings in *trans* positions. Slightly different metrics (see ESI†) and a different conformation of the coordinated EtOH make the nearly *meso* complex not exactly centrosymmetric. However, the space group is centrosymmetric with inversion centres residing between molecules. The deprotonated alkoxo (or alkoxido) oxygen atoms of the two 2.21 (py)(ph)CH(O)$^-$ ligands doubly bridge the two metal centres. The In1···In2 distance is relatively short [3.459(1) Å] due to the presence of two monoatomic bridges. Each bridge is nearly symmetrical; for example the In1–O2 and In2–O2 distances are 2.134(3) and 2.161(3) Å, respectively. The In–O–In angles are ~107°. The central $\{In^{III}_2(\mu\text{-}OR)_2\}^{4+}$ core [R- = (py)(ph)CH-] can be described as approximately rhombic. However, the four sides of the "rhombus" are not equal [2.134(3)–2.184(3) Å]; furthermore, the two In^{III} and the two bridging alkoxo oxygen atoms are not strictly coplanar with torsion angles of ~1.9°. The large diagonal of the "rhombus" is 3.459(1) Å, while the short one is 2.565(1) Å. At each In^{III} atom, two terminal bromo atoms, the pyridyl nitrogen atom of one ligand and the oxygen atom of one terminal EtOH molecule complete 6-coordination. The In^{III}–Br bond lengths [2.532(1)–2.622(1) Å] are similar with those in **3** which also contains only terminal bromides. The In^{III}–O_{alkoxo} bonds are stronger than the In^{III}–O_{EtOH} ones, as expected. The indium(III) coordination geometries are distorted octahedral, the *trans* angles being in the ranges 144.4(1)–172.6(1)° and 145.2(1)–173.6(1)° for In1 and In2, respectively. For both metal ions, the *trans* pairs of donor atoms are defined by Br, O_{alkoxo}, Br, O_{EtOH} and O_{alkoxo}, N. There are two weak intramolecular H bonds (Fig. S5†). The donor atoms are the EtOH oxygens O3 and O4, and the acceptors are the bromo groups Br4 and Br2, respectively; the donor and acceptor atoms of each H bond belong to the coordination sphere of different metal ions [for example, O4···Br2 = 3.279(2) Å and O4–H(O4)···Br2 = 178.8°]. A consequence of these H bonds is

Table 1 Crystallographically characterised metal complexes that contain various transformed ligands or counterions derived from the creativity of coordinated (py)(ph)CO

Compound[a,b]	Ref.
$\{(L)[Cu^II_2]\}_n$ [c]	15*a*
$\{(L)[Cu^I(SCN)_2]\}_n$ [c]	15*b*
$[Ru^{II}Cl\{(py)CO_2\}(CO)(PPh_3)_2]$	15*c*
$[Re^{V}OX_2\{(py)(ph)CH(O)\}(PPh_3)]$[d]	15*d* and *g*
$[Cu^{II}_2\{(py)(ph)C(OH)(O)\}_2\{(py)(ph)CO\}_2(H_2O)](ClO_4)_2$	15*e* and *f*
$[Sn^{II}(L')\{(py)(ph)CH(O)\}]$	15*h*
$[Cu^{II}_2\{(py)(ph)C(OMe)(O)\}_2\{(py)(ph)CO\}_2](ClO_4)_2$	16*a*
$[Cu^{II}_4(OMe)_2(NO_3)_4\{(py)(ph)C(OMe)(O)\}_2\{(py)(ph)CO\}_2]$	16*a*
$[Cu^{II}_2(NO_3)_2\{(py)(ph)C(OEt)(O)\}_2(EtOH)]$	16*a*
$[Cu^{II}_2(NO_3)_2\{(py)(ph)C(CH_2NO_2)(O)\}_2]$	16*a*
$[Ni^{II}\{(py)(ph)C(CH_2CN)(O)\}_2]$	16*b*
$[In_2Br_4\{(py)(ph)CH(O)\}_2(EtOH)_2]$ (**4**)	This work
$(L)[InBr_4\{(py)(ph)CO\}]$ (**3**)[c]	This work

[a] Lattice solvent molecules have been omitted. [b] For the structural formulae of the transformed ligands and their coordination modes, see Scheme 5. [c] L^+ is the uncoordinated counterion 9-oxo-indolo[1,2-*a*]pyridinium, whose structural formula is also shown in Scheme 5. [d] X = Cl, Br. $(L')^-$ is $HC\{CMeN(2,6\text{-}{}^iPr_2C_6H_3)_2\}^-$ with ^iPr representing the isopropyl group.

 This journal is © The Royal Society of Chemistry 2022

Open Access Article. Published on 28 2022. Downloaded on 5.11.2024 . 13:44:01.
This article is licensed under a Creative Commons Attribution 3.0 Unported Licence.

that the In^{III}–Br bond lengths involving the H-bonded bromo atoms [In1–Br2 = 2.614(1) and In2–Br4 = 2.622(1) Å] are longer (*i.e.* weaker) than those involving the "free" ones [In1–Br1 = 2.537(1) and In2–Br3 = 2.532(1) Å]. The C6–O1 and C18–O2 bond lengths are identical [1.406(6/5) Å] and this value is typical[17] for single carbon–oxygen bonds, confirming the reduction at the carbonyl group of (py)(ph)CO to (py)(ph)CH(O)$^-$. These bond distances are almost identical with those seen in complexes containing the (py)(ph)CH(O)$^-$ ligand;[15d,g,h] for example, this bond length is 1.40(2) Å in complex [Sn^{II}(L′){(py)(ph)CH(O)}],[15h] where (L′)$^-$ is HC{CMeN(2,6-^{i}Pr$_2$C$_6$H$_3$)$_2$}$^-$.

Weak intermolecular $C_{aromatic}$–H···Br interactions are present in the structure of **4** (C···Br = 3.80–3.83 Å), forming an 1D network in the crystal (Fig. 4).

Complex **4** is the first structurally characterised In(III) complex with the neutral or anionic form of (py)(ph)CH(OH) as ligand. It joins a small family of metal complexes with (py)(ph)C(H)(OH)[26] or (py)(ph)CH(O)$^-$;[15d,g,h,26,27] three of them (Table 1) have been derived by reactivity studies of coordinated (py)(ph)CO.[15d,g,h] The neutral molecule behaves as a N,O-chelating ligand (1.11),[26] while the anionic ligand acts in the 1.11,[15d,g] 1.01[15h] or 2.21[26,27] manner.

Spectroscopic discussion in brief

Data are shown in Fig. 5, 6 and S1, S6–S17.† In the IR spectra of **1** (Fig. S6†) and **4**, the weak-to-medium intensity bands at ~3440 and ~3320 cm^{-1}, respectively, are assigned to the ν(OH) vibration of the coordinated EtOH molecules;[16a] their relatively low wavenumber and broadness are both indicative of H bonding (established by crystallography). The presence of EtOH is manifested by the appearance of the signals at δ ~1.1 (–CH_3), ~3.5 (–CH_2) and ~4.35 (–OH) ppm (Fig. S7†). The IR spectra of **1** and **3** (Fig. S8†) exhibit a strong-to-medium intensity band at ~1625 cm^{-1} attributed to the ν(C=O) of the ligated (py)(ph)CO;[16a] due to coordination, this band has been shifted to a lower wavenumber compared with the corresponding vibration in the spectrum of free (py)(ph)CO at 1668 cm^{-1} (Fig. S9†).[28] The corresponding Raman peak

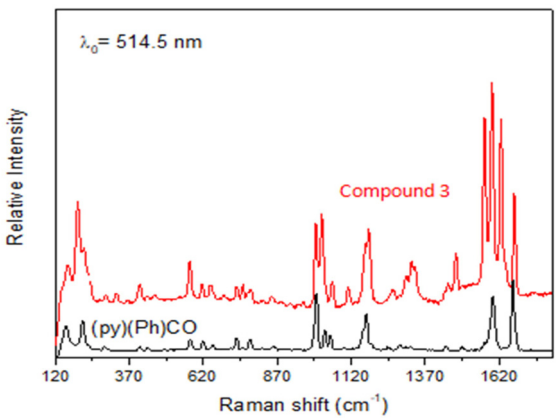

Fig. 5 The Raman spectra (cm^{-1}) of free (py)(ph)CO (bottom) and compound (L)[$InBr_4${(py)(ph)CO}] (**3**).

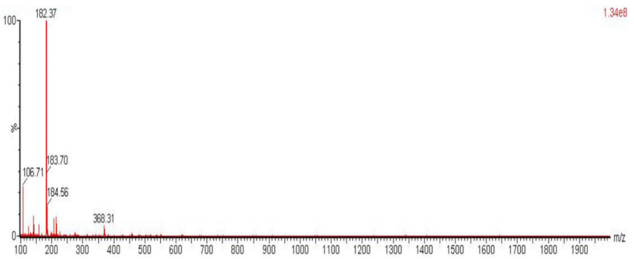

Fig. 6 The ESI-MS spectrum of {(pyH)(ph)CO}Cl (**2**) in the positive mode.

appears at 1626 (**1**), 1628 (**3**) and 1665 [free (py)(ph)CO] cm^{-1} (Fig. 5 and S10†). The IR spectra of **1** and **3** show an additional carbonyl stretching vibration at 1668 cm^{-1}. These can be undoubtedly assigned to the ν(C=O) vibration of the lattice (py)(ph)CO molecule that is present in **1** and the L$^+$ (Scheme 2) ion which counterbalances the charge of [$InBr_4${(py)(ph)CO}]$^-$ in compound **3**. The corresponding Raman peaks appear at 1671 (**1**) and 1670 (**3**) cm^{-1}. Thus, vibrational spectroscopy can easily reflect the two different carbonyl groups in each of these two complexes. The IR spectrum of **4** does not display a band in the carbonyl stretching vibration region (1730–1620 cm^{-1}) region, in accordance with the reduction of the carbonyl group (*i.e.* absence of $\nu_{C=O}$) in this dinuclear complex; the nearest band at 1608 cm^{-1} in the spectrum of **4** is due to an aromatic stretching vibration. The medium intensity IR band at 1082 cm^{-1} can be assigned[29,30] to the stretching vibration of the single carbon–oxygen bond, ν(C–O), of the ligand. The Raman peaks of **1** at 233 cm^{-1} and **3** at 196 cm^{-1} are attributed to a stretching vibration of the terminal In^{III}–Cl, $\nu(In–Cl)_t$, and In^{III}–Br, $\nu(In–Br)_t$, respectively;[17,31] both peaks are absent from the spectrum of free (py)(ph)CO, as expected.

The behavior of **1**, **3** and **4** in solution (DMSO) was probed by ^{1}H NMR spectroscopy. The spectrum of **1** in d_6-DMSO (Fig. S7†) shows, in addition to the EtOH signals, all the signals of free (py)(ph)CO (Fig. S11†) at exactly the same δ values. This, together with the negligible value of the molar conductivity (Λ_M) of **1** in DMSO (3 S cm^2 mol^{-1}),[32] indicates decomposition of the complex in solution to release free (py)(ph)CO, eqn (1).

$$\underset{\mathbf{1}}{[InCl_3\{(py)(ph)CO\}(EtOH)]}\{(py)(ph)CO\} + 3DMSO \xrightarrow{DMSO} [InCl_3(DMSO)_3] + 2(py)(ph)CO \quad (1)$$

The ^{1}H NMR spectrum of **3** in d_6-DMSO is a sum of signals arising from the cation L$^+$ and free (py)(ph)CO. The Λ_M value in DMSO (36 S cm^2 mol^{-1}) is indicative of an 1 : 1 electrolyte, again suggesting decomposition in solution, eqn (2).

$$(L)\underset{\mathbf{3}}{[InBr_4\{(py)(ph)CO\}]} + 2DMSO \xrightarrow{DMSO} (L)^+ + [InBr_4(DMSO)_2]^- + (py)(ph)CO \quad (2)$$

In addition to the typical EtOH signals, the ^{1}H NMR spectrum of **4** (Fig. S12†) shows the typical signals of free (py)(ph)CO. This was a surprise because the complex contains the

Open Access Article. Published on 28 2022. Downloaded on 5.11.2024 . 13:44:01.
This article is licensed under a Creative Commons Attribution 3.0 Unported Licence.

reduced form of 2-benzoylpyridine, *i.e.* the anionic ligand (py)(ph)CH(O)$^-$. We anticipated the appearance of a singlet in the δ range 4.5–6.5 ppm attributable[14e,15h,33] to the quaternary CH proton of the reduced ligand; such a signal could not be seen in more than ten samples of **4**. The only explanation we can offer is the aerobic oxidation of (py)(ph)CH(O)$^-$, catalyzed by In(III), in the presence of oxygen. This reaction with Co$(O_2CMe)_2{\cdot}4H_2O$ as catalyst is well documented.[27b] It is interesting to note that these catalytic aerobic oxidation reactions are very selective to pyridine-based secondary alcohols, such as (py)(ph)CH(OH), over primary alcohols and that they take place without any external ligand, base or additive.[27b] Compound **2** (*vide supra*) was identified as the hydrochloride salt of 2-benzoylpyridine, {(pyH)(ph)CO}Cl, by microanalyses, physical techniques and spectroscopic methods. A $AgNO_3$ test for an acidic sample of the compound is positive for Cl^- ions. Its melting/decomposition point is 168 °C, much higher than that of the free (py)(ph)CO (42–43 °C). The Λ_M value (38 S cm^2 mol^{-1}) in DMSO indicates an 1 : 1 electrolyte in solution. In the IR spectrum (Fig. S13†), the bands at ~2850 and 1738 cm^{-1} are assigned to the ν(NH$^+$) and ν(C=O) vibrations, respectively. The high wavenumber of ν(C=O) reflects the –I inductive effect of the positive N atom on the carbonyl group. The ^{1}H NMR spectrum of **2** (Fig. S14†) is pretty similar with that of free (py)(ph)CO, with the only essential difference being the doublet at δ 8.49 ppm in the spectrum of the former which is attributed to the NH$^+$ proton. The aromatic proton signals appear at the same δ values in the two spectra; this is most probably due to the existence of a strong five-membered intramolecular N–H···O$_{carbonyl}$ H bond, mentioned in the explanation of the mechanism detailed in Scheme 3. For the same reason, the $^{13}C\{^1H\}$ NMR spectra of (py)(ph)CO (Fig. S15†) and **2** (Fig. S16†) are also very similar. A definite proof for the identity of this compound comes from mass spectrometry (Fig. 6 and S17†). The ESI-MS spectrum of the compound in the positive mode shows the expected [M + H]$^+$ quasi-molecular ion at *m*/*z* 184.56 and an associated fragment at *m*/*z* 106.70 ([PhCHO]$^+$), but also the [M]$^+$ molecular ion at *m*/*z* 183.70. However, the strongest peak by far is at *m*/*z* 182.37 attributed to [M − 1]$^+$, whose structure is probably identical with that of the cation L$^+$ of the salt (L)$^+$Br$^-$ (Scheme 4); this is formed from the molecular ion (radical cation) with a H atom loss. On the other hand, the ESI-MS spectrum of the same compound in the negative mode provides strong evidence in favour of the hydrochloride salt **2**. Indeed, the quasi-molecular ion is observed at *m*/*z* 259.22, 257.23 and 255.23, which corresponds to the cluster [**2** + HCl]$^-$ formed by an one-electron reduction of **2** and uptake of one HCl molecule.[34]

Concluding comments

In this work, we have reported that the employment of (py)(ph)CO in reactions with $InBr_3$ has resulted in interesting transformations of the ligand, demonstrating that metal ion-driven reactivity of 2-pyridyl ketones remains an interesting area of research. The complex salt **3** is the third structurally characterised compound containing the cation L$^+$ (Table 1), while compound **4** is the fourth structurally characterised complex possessing the reduced anionic ligand (py)(ph)CH(O)$^-$ arising from (py)(ph)CO (Table 1). Mechanistic schemes have been proposed for the observed transformations (Scheme 4) in **3** and **4**, and for the byproduct **2**. Since all the previous examples on the reactivity of coordinated (py)(ph)CO were with transition metals, our results show that transformations are also possible with p-block elements. Although compound (py)(ph)CH(OH) can be prepared by metal ion-free reduction of (py)(ph)CO,[20] the observed (py)(ph)CO → **4** (this work) and (py)(ph)CO → [Re^{V}OX$_2${(py)(ph)CH(O)}(PPh$_3$)][15d,g] transformations show that this reaction can be also metal ion-assisted. Overall compounds **1**, **3** and **4** are the first In(III) complexes derived from (py)(ph)CO or (py)(ph)CO-based species.

A comparison between the reactivity of coordinated (py)(ph)CO (Scheme 2) and $(py)_2CO$ (Scheme 1) reveals that the formation of L$^+$ has been observed only for the former (ref. 15*d*, *g* and this work). On the contrary, the ligand $(py)_2CH(O)^-$ has been derived from the Ni^{II}-promoted reduction of $(py)_2CO$ under solvothermal conditions.[35]

The question of why $InCl_3$ does not provide L$^+$ or (py)(ph)CH(O)$^-$ (whereas $InBr_3$ does), under identical reaction conditions, is difficult to be answered without DFT calculations. Differences in the products of reactions of $InCl_3$ and $InBr_3$ with simple ligands are often observed, even from the early years of the development of In(III) chemistry.[36] Lattice energies of the products have been proposed as the reason of the differences. Based on this assumption, it is possible that transformed species are present in the reaction $InCl_3$/(py)(ph)CO solutions in EtOH and that the more insoluble compounds **1** and **2** are preferentially precipitated. Using a more chemical basis, it is well known[37] that ligand reactivity is affected by three factors: (a) the electron-acceptor/donor properties of the metal centre; (b) the electron-donor/acceptor properties of the ligands; and (c) the nature of the co-ligands. In our case, only factor *c* is variable. We believe that the slightly different net electron donor/acceptor abilities of chlorides and bromides are an explanation for the observed differences. Perhaps, the Br$^-$ co-ligand has a net electron donor/acceptor ability more opposite (compared to the Cl$^-$ one) to that of (py)(ph)CO, thus assisting In(III) towards activation of the primary organic ligand;[37] if this hypothesis is valid, the chloride and (py)(ph)CO have similar electronic ability, they complete each other and feel a reduced activation by the metal centre.

We do believe that this particular research topic has more interesting results to give. We continue to investigate the reactivity of other activated compounds containing carbonyl groups (ketones and aldehydes) and metal-mediated synthesis, and we expect further advances not only in stoichiometric reactions but also, more importantly, in catalysis. Our current efforts involve: (i) reactions of the other trivalent metals of group 13, *e.g.* Al(III) and Ga(III), with (py)(ph)CO; and (ii) replacement of the phenyl ring of (py)(ph)CO with a methyl group (*i.e.*, use of 2-acetylpyridine) which is less bulky, has an

 This journal is © The Royal Society of Chemistry 2022

Open Access Article. Published on 28 2022. Downloaded on 5.11.2024 . 13:44:01.
This article is licensed under a Creative Commons Attribution 3.0 Unported Licence.

opposite inductive effect and contains polar C–H bonds adjacent to the carbonyl group (*i.e.* weakly acidic α-hydrogens), all these characteristics giving hopes[16a] for interesting reactivity patterns with group 13 and other p-block metals. Preliminary results with Ga(III) concerning point (ii) reveal the formation of the coordinated ligand (py)C(Me)(OH)CH_2C(OMe)(O)(py)$^-$, a transformation which has been reported previously in Cu(II) chemistry.[16a] As a final note, we plan to include advanced theoretical calculations to more rigorously explain the experimental facts and the observed differences in the reactivity patterns of similar systems.

Author contributions

CS: investigation, data curation, formal analysis. ZGL: data curation, formal analysis, validation. CTC: data curation, formal analysis. DP: conceptualisation, supervision, writing – review and editing, writing manuscript. PD: data curation, investigation, formal analysis, writing review and editing, writing manuscript. SPP: conceptualisation, supervision, project management, writing manuscript.

Conflicts of interest

There are no conflicts to declare.

Acknowledgements

We thank Research Director George Voyiatzis for permitting us to use the Raman facilities at ICE-HT/FORTH and Dr Vlasoula Bekiari for recording the emission spectrum of complex **4** at the Department of Crop Science of the University of Patras (Messolonghi campus).

References

1 E. C. Constable, *Metals and Ligand Reactivity*, VCH, Weinheim, Germany, 1996, pp. 22–62.
2 G. L. Miessler, P. J. Fischer and D. A. Tarr, *Inorganic Chemistry*, Pearson, Boston, USA, 5th edn, 2014, pp. 468–470.
3 D. Sun, D.-F. Wang, N. Zhang, F.-J. Liu, H.-J. Hao, R.-B. Huang and L.-S. Zheng, *Dalton Trans.*, 2011, **40**, 5677–5679.
4 M. Riaz, R. K. Gupta, H.-F. Su, Z. Jagličic, M. Kurmoo, C.-H. Tung, D. Sun and L.-S. Zheng, *Inorg. Chem.*, 2019, **58**, 14331–14337.
5 Y.-Q. Zhao, M.-X. Fang, Z.-H. Xu, X.-P. Wang, S.-N. Wang, L.-L. Han, X.-Y. Li and D. Sun, *CrystEngComm*, 2014, **16**, 3015–3019.
6 B. Liu, F. Yu, M. Tu, Z.-H. Zhu, Y. Zhang, Z.-W. Ouyang, Z. Wang and M.-H. Zeng, *Angew. Chem., Int. Ed.*, 2019, **58**, 3748–3753.
7 Z.-H. Zhu, Q. Hu, H.-L. Pan, Y. Zhang, H. Xu, M. Kurmoo, J. Huang and M.-H. Zeng, *Sci. China: Chem.*, 2019, **62**, 719–726.
8 R. W. Hay, in *Reactions of Coordinated Ligands*, ed. P. S. Braterman, Plenum, New York, USA, 1989, vol. 2.
9 R. W. Hay, in *Comprehensive Coordination Chemistry I*, ed. G. Wilkinson, R. D. Gillard and J. A. McCleverty, Pergamon, Oxford, 1987, vol. 6.
10 For older reviews, see: (*a*) G. S. Papaefstathiou and S. P. Perlepes, *Comments Inorg. Chem.*, 2002, **23**, 249–274; (*b*) A. J. Tasiopoulos and S. P. Perlepes, *Dalton Trans.*, 2008, 5537–5555 (perspective); (*c*) T. C. Stamatatos, C. G. Efthymiou, C. C. Stoumpos and S. P. Perlepes, *Eur. J. Inorg. Chem.*, 2009, 3361–3391 (microreview).
11 T. C. Stamatatos, S. P. Perlepes, C. P. Raptopoulou, A. Terzis, C. S. Patrickios, A. J. Tasiopoulos and A. K. Boudalis, *Dalton Trans.*, 2009, 3354–3362.
12 Representative examples: (*a*) G. S. Papaefstathiou, C. P. Raptopoulou, A. Tsohos, A. Terzis, E. G. Bakalbassis and S. P. Perlepes, *Inorg. Chem.*, 2000, **39**, 4658–4662; (*b*) T. C. Stamatatos, S. P. Perlepes, C. P. Raptopoulou, V. Psycharis, C. S. Patrickios, A. J. Tasiopoulos and A. K. Boudalis, *Inorg. Chem. Commun.*, 2009, **12**, 402–405.
13 Representative examples from our group: (*a*) C. C. Stoumpos, O. Roubeau, G. Aromi, A. J. Tasiopoulos, V. Nastopoulos, A. Escuer and S. P. Perlepes, *Inorg. Chem.*, 2010, **49**, 359–361; (*b*) C. G. Efthymiou, C. Papatriantafyllopoulou, G. Aromi, S. J. Teat, G. Christou and S. P. Perlepes, *Polyhedron*, 2011, **30**, 3022–3025; (*c*) C. G. Efthymiou, I. Mylonas-Margaritis, C. P. Raptopoulou, V. Psycharis, A. Escuer, C. Papatriantafyllopoulou and S. P. Perlepes, *Magnetochemistry*, 2016, **2**, 30; (*d*) Z. G. Lada, Y. Sanakis, C. P. Raptopoulou, V. Psycharis, S. P. Perlepes and G. Mitrikas, *Dalton Trans.*, 2017, **46**, 8458–8475; (*e*) C. C. Stoumpos, P. Danelli, G. Zahariou, M. Pissas, V. Psycharis, C. P. Raptopoulou, Y. Sanakis and S. P. Perlepes, *Polyhedron*, 2021, **207**, 115350; (*f*) K. Skordi, A. Anastasiades, A. D. Fournet, R. Kumar, M. Schulze, W. Wernsdorfer, G. Christou, V. Nastopoulos, S. P. Perlepes, C. Papatriantafyllopoulou and A. J. Tasiopoulos, *Chem. Commun.*, 2021, **57**, 12484–12487.
14 For example, see: (*a*) B. Machura, J. Palion, J. Mrozinski, B. Kalinska and R. Kruszynski, *Polyhedron*, 2013, **49**, 216–222; (*b*) B. Machura, I. Nawrot, K. Michalik and Z. Drzazga, *Polyhedron*, 2011, **30**, 2294–2302; (*c*) C. J. Milios, T. C. Stamatatos, P. Kyritsis, A. Terzis, C. P. Raptopoulou, R. Vicente, A. Escuer and S. P. Perlepes, *Eur. J. Inorg. Chem.*, 2004, 2885–2901; (*d*) A. Schneider and H. Vahrenkamp, *Z. Anorg. Allg. Chem.*, 2003, **629**, 2122–2126; (*e*) C. Sudbrake and H. Vahrenkamp, *Inorg. Chim. Acta*, 2001, **318**, 23–30.
15 (*a*) M. A. S. Goher, A. E. H. Abdou, B.-S. Luo and T. C. W. Mak, *J. Coord. Chem.*, 1995, **36**, 71–80; (*b*) M. A. S. Goher, R.-J. Wang and T. C. W. Mak, *J. Coord. Chem.*, 1996, **38**, 151–154; (*c*) J. G. Malecki and R. Kruszynski, *Polyhedron*, 2007, **26**, 2686–2694;

Open Access Article. Published on 28 2022. Downloaded on 5.11.2024 . 13:44:01.
This article is licensed under a Creative Commons Attribution 3.0 Unported Licence.

(*d*) B. Machura, J. Milek, R. Kruszynski, J. Kusz and J. Mrozinski, *Polyhedron*, 2008, **27**, 1262–1269; (*e*) S. Dey, S. Sarkar, E. Zangrando, H. Stoeckli Evans, J.-P. Sutter and P. Chattopadhyay, *Inorg. Chim. Acta*, 2011, **367**, 1–8; (*f*) Y. Li and L. Jin, *J. Cluster Sci.*, 2011, **22**, 41–47; (*g*) N. C. Yumata, G. Habarurema, J. Mukiza, T. I. A. Gerber, E. Hosten, F. Taherkhani and M. Nahali, *Polyhedron*, 2013, **62**, 89–103; (*h*) A. Jana, H. W. Roesky, C. Schulzke and A. Doring, *Angew. Chem., Int. Ed.*, 2009, **48**, 1106–1109.

16 (*a*) A. A. Kitos, C. G. Efthymiou, M. J. Manos, A. J. Tasiopoulos, V. Nastopoulos, A. Escuer and S. P. Perlepes, *Dalton Trans.*, 2016, **45**, 1063–1077; (*b*) A. A. Kitos, D. P. Giannopoulos, C. Papatriantafyllopoulou, L. Cunha-Silva and S. P. Perlepes, *Inorg. Chem. Commun.*, 2016, **64**, 53–55.

17 C. Stamou, W. Papawassiliou, J. P. Carvalho, K. F. Konidaris, V. Bekiari, P. Dechambenoit, A. J. Pell and S. P. Perlepes, *Inorg. Chem.*, 2021, **60**, 4829–4840.

18 (*a*) F. J. Alguacil, *Molecules*, 2020, **25**, 5238; (*b*) C. E. Housecroft and A. G. Sharpe, *Inorganic Chemistry*, Pearson, Harlow, UK, 5th edn, 2018, p. 391; (*c*) R. Kaiukov, G. Almeida, S. Marras, Z. Dang, D. Baranov, U. Petralanda, I. Infante, E. Mugnaioli, A. Griesi, L. De Trizio, M. Gemmi and L. Manna, *Inorg. Chem.*, 2020, **59**, 548–554; (*d*) J. Liang, X. Han, J.-H. Yang, B. Zhang, Q. Fang, J. Zhang, Q. Ai, M. M. Ogle, T. Terlier, A. A. Marti and J. Lou, *Adv. Mater.*, 2019, **31**, 1903448; (*e*) Y. Huang, T.-K. Jiang, B.-P. Yang, C.-L. Hu, Z. Fang and J.-G. Mao, *Inorg. Chem.*, 2022, **61**, 3374–3378.

19 (*a*) Y.-Z. Li, G.-D. Wang, Y.-K. Lu, L. Hou, Y.-Y. Wang and Z. Zhu, *Inorg. Chem.*, 2020, **59**, 15302–15311; (*b*) C. Lu, D. Xiong, C. Chen, J. Wang, Y. Kong, T. Liu, S. Ying and F.-Y. Yi, *Inorg. Chem.*, 2022, **61**, 2587–2594; (*c*) S. Dagorne, M. Normand, E. Kirillov and J.-F. Carpentier, *Coord. Chem. Rev.*, 2013, **257**, 1869–1886; (*d*) G.-M. Liang, P. Xiong, K. Azam, Q.-L. Ni, J.-Q. Zeng, L. C. Gui and X.-J. Wang, *Inorg. Chem.*, 2020, **59**, 1653–1659; (*e*) M. Gut and J. P. Holland, *Inorg. Chem.*, 2019, **58**, 12302–12310; (*f*) M. R. Gill, M. G. Walker, S. Able, O. Tietz, A. Lakshminarayanan, R. Anderson, R. Chalk, A. H. El-Sagheer, T. Brown, J. A. Thomas and K. A. Vallis, *Chem. Sci.*, 2020, **11**, 8936–8944; (*g*) D. V. Wagle, S. P. Kelley, G. A. Baker, K. Sikligar and J. L. Atwood, *Angew. Chem., Int. Ed.*, 2020, **59**, 8062–8065; (*h*) F. Chen, G. Ma, G. M. Bernard, R. G. Cavell, R. McDonald, M. J. Ferguson and R. E. Wasylishen, *J. Am. Chem. Soc.*, 2010, **132**, 5479–5493; (*i*) S. Banerjee, S. Dutta, S. Kumar Sarkar, N. Graw, R. Herbst-Irmer, D. Koley, D. Stalke and H. W. Roesky, *Dalton Trans.*, 2020, **49**, 14231–14236; (*j*) K. Zeckert and D. Fuhrmann, *Inorg. Chem.*, 2019, **58**, 16736–16742.

20 H. Kim and S. K. Kang, *Acta Crystallogr., Sect. E: Struct. Rep. Online*, 2014, **70**, o947.

21 G. M. Sheldrick, *SADABS, ver. 2.03*, Bruker Analytical X-Ray Systems, Madison, WI, USA, 2000.

22 (*a*) G. M. Sheldrick, *Acta Crystallogr., Sect. A: Found. Adv.*, 2015, **71**, 3–8; (*b*) G. M. Sheldrick, *Acta Crystallogr., Sect. C: Struct. Chem.*, 2015, **71**, 3–8.

23 R. A. Coxall, S. G. Harris, D. K. Henderson, S. Parsons, P. A. Tasker and R. E. P. Winpenny, *J. Chem. Soc., Dalton Trans.*, 2000, 2349–2355.

24 C. Birnara, V. G. Kessler and G. S. Papaefstathiou, *J. Coord. Chem.*, 2017, **70**, 1–20.

25 M. Sievert, R. Dinelt and H. Bock, *Acta Crystallogr., Sect. C: Cryst. Struct. Commun.*, 1998, **54**, 674–676.

26 F. Di Salvo, M. Y. Tsang, F. Teixidor, C. Viñas, J. G. Planas, J. Crassous, N. Vanthuyne, N. Aliaga-Alcalde, E. Ruiz, G. Coquerel, S. Clevers, V. Dupray, D. Choquesillo-Lazarte, M. Light and M. B. Hursthouse, *Chem. – Eur. J.*, 2014, **20**, 1081–1090.

27 (*a*) Z. Hao, N. Li, X. Yan, Y. Li, S. Zong, H. Liu, Z. Han and J. Lin, *New J. Chem.*, 2018, **42**, 6968–6975; (*b*) I. Karthikeyan, S. K. Alamsetti and G. Sekar, *Organometallics*, 2014, **33**, 1665–1671; (*c*) W.-Q. Chen, Y.-M. Chen, T. Lei, W. Liu and Y. Li, *Inorg. Chem. Commun.*, 2012, **19**, 4–9; (*d*) A. Schneider and H. Vahrenkamp, *Z. Anorg. Allg. Chem.*, 2004, **630**, 1059–1061.

28 T. M. Kolev and P. Bleckmann, *Spectrosc. Lett.*, 1989, **22**, 1215–1227.

29 L. J. Bellamy, *The Infra-red Spectra of Complex Molecules*, Methuen, London, UK, 2nd edn, 1966, pp. 108–111.

30 C. N. R. Rao, *Chemical Applications of Infrared Spectroscopy*, Academic Press, New York, USA, 1963, pp. 175–188.

31 D. M. Adams, *Metal-Ligand and Related Vibrations*, Arnold, London, UK, 1967, pp. 26–79.

32 W. J. Geary, *Coord. Chem. Rev.*, 1971, **7**, 81–122.

33 Z. Hao, N. Li, X. Yan, X. Yue, K. Liu, H. Liu, Z. Han and J. Lin, *J. Organomet. Chem.*, 2018, **870**, 51–57.

34 N. B. Lentz and R. S. Houk, *J. Am. Soc. Mass Spectrom.*, 2007, **18**, 285–293.

35 C. G. Efthymiou, T. C. Stamatatos, C. Papatriantafyllopoulou, A. J. Tasiopoulos, W. Wernsdorfer, S. P. Perlepes and G. Christou, *Inorg. Chem.*, 2010, **49**, 9737–9739.

36 A. J. Carty, *Can. J. Chem.*, 1967, **45**, 345–351.

37 A. J. L. Pombeiro and V. Yu. Kukushkin, in *Comprehensive Coordination Chemistry II*, ed. J. A. McCleverty and T. J. Meyer, Elsevier, Amsterdam, The Netherlands, 2004, vol. 1, pp. 585–594.

This journal is © The Royal Society of Chemistry 2022